

# NiCrWRe 喷熔层组织和耐磨特性

张振宇<sup>1,2</sup>, 王智平<sup>2</sup>, 梁补女<sup>1</sup>

(1. 兰州工业高等专科学校 机械工程系, 兰州 730050;

2. 兰州理工大学 有色金属新材料国家重点实验室, 兰州 730050)

**摘 要:** 采用火焰喷熔方法在 45 钢表面制取了 NiCrWRe 喷熔层, 并与 NiCrW 合金喷熔层进行耐磨对比试验。利用 XRD 分析了喷熔层的相结构, 用 SEM 和 EDS 等技术分析了喷熔层的表面、截面及磨损面形貌, 测定了与基体的结合力。结果表明, NiCrWRe 喷熔层组织均匀细化。稀土元素促进了喷熔层和基体之间原子的扩散, NiCrWRe 喷熔层与基体 45 号钢形成了牢固的冶金结合, 提高了喷熔层结合强度。同时还含有较高比例的硬质相; 稀土的加入使喷熔层的耐磨性显著提高, 在给定的试验条件下, NiCrWRe 涂层的耐磨性明显高于 NiCrW。

**关键词:** 稀土; 喷熔层; 磨粒磨损; 耐磨性

中图分类号: TG174.442 文献标识码: A 文章编号: 0253-360X(2007)09-025-04



张振宇

## 0 序 言

火焰喷熔是表面工程中广泛应用的表面改性技术, 且工艺简单易行, 除可强化工件表面外, 还兼有修复旧件之功能, 并通过改变合金粉末成分可在较大范围内改变喷熔层的性能<sup>[1,2]</sup>。自熔性合金火焰喷熔使用的材料包括钴基、铁基、镍基及铜基四大类。根据抗磨粒磨损工件的要求和不同粉末本身的特性, 在生产中应用最为广泛的耐磨粒磨损喷熔层的材料主要采用镍铬硼硅系和镍铬硼硅加碳化钨系两类自熔性合金。近年来, 镍基、钴基和铁基等自熔性合金涂层被广泛应用于材料表面保护及工件修复, 特别是在大型进口设备的维修及关键部件的替代方面, 具有明显的经济效益和社会效益。镍基自熔性合金具有优良的耐磨、耐热和抗氧化性能, 因而镍基合金应用更加广泛<sup>[3]</sup>。

稀土元素因其具有特殊的电子结构和物理化学性质, 在材料科学领域得到了广泛的应用。近年来稀土在摩擦学材料中的应用也得到了重视。镍基合金具有优良的力学和高温抗氧化性能, 已广泛应用于零件表面的强化和防护。稀土已成功应用到热喷涂、喷熔及激光熔覆中, 在涂层的微观结构、耐磨耐蚀性能等方面的影响在有关文献[4-7]中作了报道, 且大部分是复合涂层中加稀土, 而稀土合金化镍基合金粉末

喷熔层的性能研究方面的报道还比较少。

## 1 试验方法

### 1.1 试样制备

采用 KJP100 (1 000 Hz) 中频感应电炉熔炼, 用钟罩将富铈混合稀土压入高温金属液中, 经过脱氧、精炼、排气、清渣后出炉, 通过惰性气体(氩气)雾化法制取 NiCrWRe 合金粉末。图 1 所示的 SEM 照片表明, 粉末颗粒球形度好, 粉末粒度分布为 40~95 μm。合金粉末的质量分数(%)为 C 1.0~2.0, Si 3.0~5.0, B 3.0~5.0, Cr 16~20, Fe ≤ 10, Re 0.2~0.6, W 3.0~5.0%, 余量为 Ni; 用 SPH-F2000 型氧-乙炔焰喷熔炬(上海喷涂机械厂产)将合金粉末均匀涂覆于经清洗、除油和喷砂(20~40 目的刚玉砂)处理后的 φ12 mm×35 mm 的 45 钢端面, 涂层厚度为 1.2 mm,

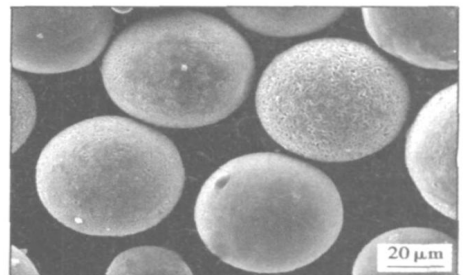


图 1 气雾化粉末形貌

Fig. 1 Powder morphology obtained by gas atomization

磨削加工后涂层的表面粗糙度为  $Ra=0.8\ \mu\text{m}$ , 试样加工成  $\phi 8\ \text{mm} \times 30\ \text{mm}$ , 加工后涂层厚度为  $0.8\ \text{mm}$ . 对比材料 NiCrW 合金的成分(质量分数, %)为 C 1.0~2.0, Si 3.0~5.0, B 3.0~5.0, Cr 16~20,  $\text{Fe} \leq 10$ , Re 0.2~0.6, W 3.0~5.0 余量为 Ni.

1.2 磨损试验

磨损试验在 RFT-III 型往复式摩擦磨损试验机上进行,  $\phi 8\ \text{mm} \times 30\ \text{mm}$  的销式试样为自制合金, 对偶件为  $70\ \text{mm} \times 13.7\ \text{mm} \times 10\ \text{mm}$  白刚玉砂条, 粒度为 180 目. 测试速度  $150\ \text{r/min}$ , 测试压力  $150\ \text{N}$ , 测试时间  $10\ \text{min}$ , 每个试样测试次数 1 500 次, 测试行程  $60\ \text{mm}$ , 室温  $20\ ^\circ\text{C}$ , 湿度 25%, 属于无润滑干摩擦试验. 磨损量用万用电子分析天平测试, 用磁选法收集磨损试验过程中的磨屑, 经过退磁后, 均匀撒在导电胶带上, 用 SEM 观察形貌, 试验细节参见文献 [8].

1.3 结合强度试验

将拉伸试样(45 号钢)中间锯断然后用 NiCrWRe 自熔性合金粉末施焊, 施焊长度不小于  $5\ \text{mm}$  (试样中间涂黑部位), 进行拉伸试验, 在微机控制的万能试验机上进行, 试验依据国家标准 GB/T228-1987《金属拉伸试验方法》, 拉伸试样见图 2.

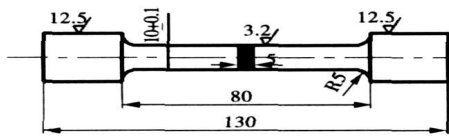


图 2 结合强度拉伸试样

Fig. 2 Bonding strength specimen

采用附带能量色散谱(EDS)的 JSM-5600LV 型扫描电子显微镜(SEM)、场发射扫描电镜(FEGSEM)和 EPMA-810Q 型电子探针观察分析合金试样的微观组织及磨损表面形貌和元素组成, 用 X'Pert PRO 型(荷兰)X 衍射仪进行物相分析, Cu 靶, 电压为  $40\ \text{kV}$ , 电流  $30\ \text{mA}$ .

2 试验结果与讨论

2.1 喷熔层组织及稀土的影响

图 3, 图 4 为 NiCrW 合金和 NiCrWRe 合金喷熔层的显微组织的 EPMA 形貌和 Ni, Cr 元素的面分布. 可以看出, 不含稀土的 NiCrW 合金喷熔层组织为粗大条状的富 Cr 组织和树枝状富 Ni 组织, 而含稀土的 NiCrWRe 合金则为细小的条状组织, 由于稀土的加入, 组织变的细小而均匀, 这是由于稀土元素易与 C, Fe 等元素生成细小固相质点而促进非自发形核, 此

外稀土元素在晶核表面的吸附作用也能阻碍晶核长大使组织明显细化<sup>[9]</sup>.

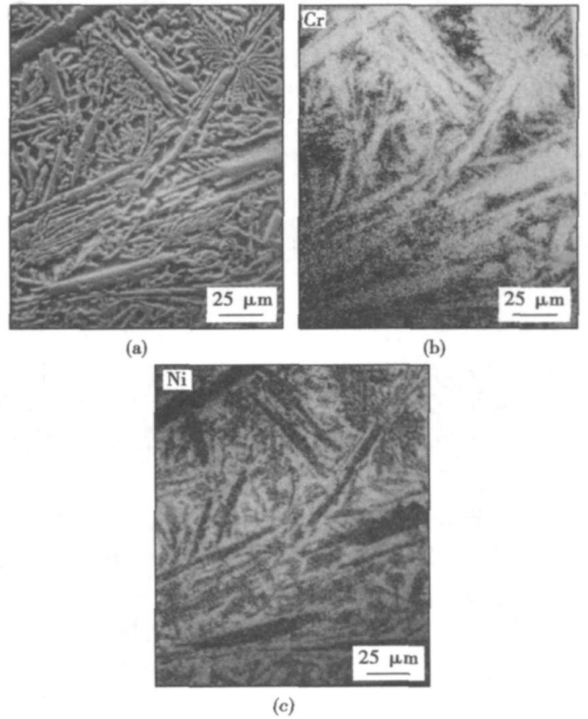


图 3 NiCrW 合金喷熔层的形貌(EPMA)和元素分布

Fig. 3 EPMA morphology and elements distribution of NiCrW alloy coatings

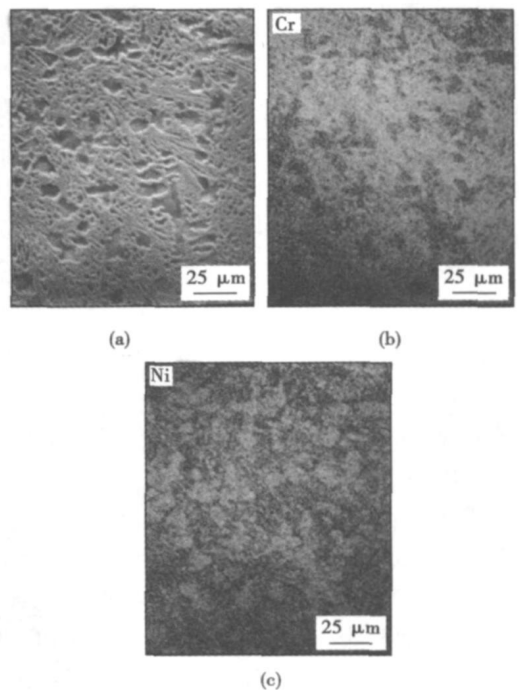


图 4 NiCrWRe 合金喷熔层的形貌(EPMA)和元素分布

Fig. 4 EPMA morphology and elements distribution of NiCrWRe alloy coatings

### 2.2 喷熔层的结合强度

表 1 为结合强度测试结果, 且试样在拉伸时从熔焊层中间断开, 其他试样拉断部位相同, 说明合金粉末与基体熔焊后形成了牢固结合, NiCrWRe 合金喷熔层的结合强度高于 NiCrW 合金喷熔层。

表 1 结合强度测试结果

Table 1 Results of bonding strength test

测试合金	试样编号	载荷 $F/kN$	抗拉强度 $R_m/MPa$
NiCrWRe	1	28.83	346
	2	26.36	323
	3	27.12	338
NiCrW	1	25.55	284
	2	24.18	296
	3	22.80	276

图 5 是喷熔层和基体界面的显微组织 FEGSEM 形貌, 可以看出, 在喷熔层和基体间过渡区域 Ni, Cr 元素的分布发生变化, 直到基体 45 号钢的正常组织, 说明在界面附近发生了明显的原子扩散, 进一步说明涂层和基体之间形成了牢固的冶金结合。由于稀土在金属液中具有强的化学活性, 增加了熔滴对基体的润湿性, 促进了熔焊层与基体之间原子的扩散, 从而提高了结合强度。

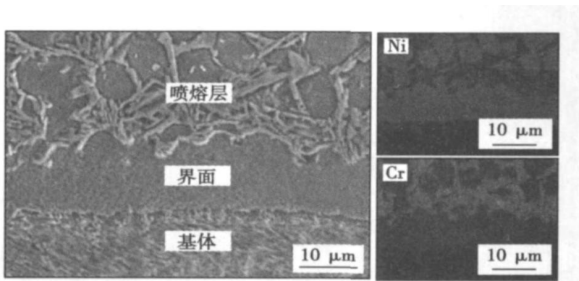


图 5 NiCrWRe 合金喷熔层断面 FEGSEM 形貌

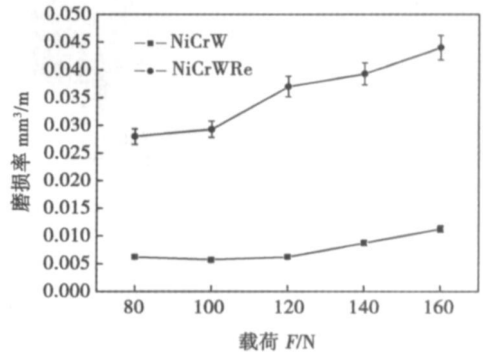
Fig. 5 FEGSEM morphology of cross section of NiCrWRe coatings

### 2.3 摩擦磨损性能

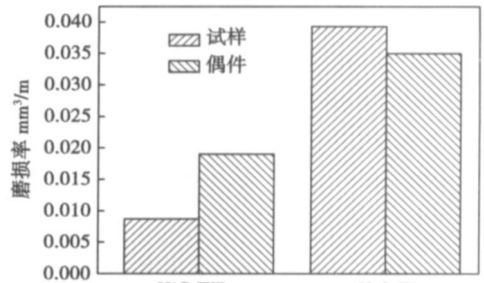
图 6a 为 NiCrWRe 和 NiCrW 合金喷熔层的磨损率变化曲线, 从中可见磨损率随着载荷的增加而增大, NiCrWRe 合金喷熔层的增幅低于 NiCrW 合金喷熔层, 且 NiCrWRe 喷熔层的磨损率小于 NiCrW 合金喷熔层。

图 6b 为载荷在 140 N 和磨损时间为 10 min 下 NiCrWRe 和 NiCrW 合金喷熔层与对偶材料的磨损率比较图。可以看出, NiCrWRe 层和对偶材料的磨损率小于 NiCrW 合金喷熔层和对偶材料, 且 NiCrWRe 喷熔

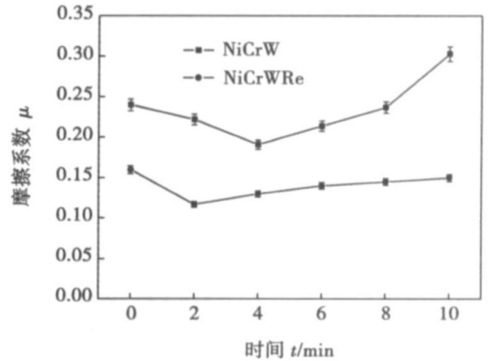
层的磨损率略低于其对偶材料, NiCrW 合金喷熔层略高于其对偶材料。



(a) 磨损率与载荷的变化曲线



(b) 试样与偶件的磨损率比较



(c) 摩擦系数变化曲线

图 6 合金喷熔层摩擦学曲线

Fig. 6 Tribological properties of alloy coatings

图 6c 为 NiCrWRe 和 NiCrW 合金喷熔层的摩擦系数变化曲线。随着时间变化, NiCrW 合金喷熔层的摩擦系数先下降, 然后上升, 而 NiCrWRe 合金喷熔层的摩擦系数变化缓慢, 趋于稳定, NiCrWRe 合金层的摩擦系数小于 NiCrW 合金喷熔层。通过对上述合金喷熔层进行的磨粒磨损试验, 含稀土的 NiCrWRe 合金喷熔层的磨损小、耐磨性好。图 7 是两种喷熔层的表面磨损形貌。相同磨损条件下, NiCrW 合金喷熔层表面划痕很深, 且有剥落发生, 磨痕宽度宽, 即磨损量大; 而 NiCrWRe 表面只出现轻微划痕。

在磨粒磨损过程中, 表面材料的磨损机制主要有三种方式<sup>[10]</sup>: (1) 显微切削; (2) 由于犁沟运动而产生

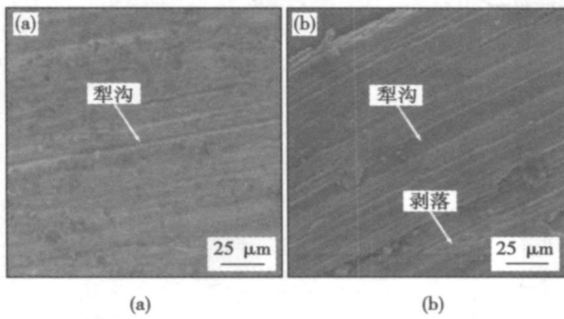


图 7 合金喷熔层表面磨损形貌 (SEM)

Fig. 7 SEM photographs of wear surface coatings

的塑性变形; (3) 弥散于基体材料中硬质相颗粒的疲劳裂纹和脱落。其中, 显微切削是磨粒磨损的主要方式。由于 NiCrWRe 合金中稀土的加入, 组织变得细化且均匀, 含 W, Cr 和 Ni 的大量硬质相分布也更加均匀, 提高了喷熔层的硬度, 抵抗了显微切削, 从而提高了合金的耐磨性, 同时, 由于适量稀土的加入, 提高了合金的力学性能, 使材料的韧性提高<sup>[7]</sup>, 稀土的加入缓解了硬度和韧性之间的矛盾。有关文献报道<sup>[10]</sup>“材料越硬越耐磨”的观点是片面的, 材料的耐磨性与硬度之间存在一定的对应关系, 也就是说, 要提高材料的耐磨性, 在提高硬度的同时还要使硬度和韧性达到最佳匹配。当磨损过程中产生的磨屑在表面与均匀弥散的硬质相碰撞, 被挤压变形时失去切削能力, 所以显微切削受到限制, 该方面的工作还有待于进一步研究。另外, 由于稀土的加入, 从 EDS 面分布看出, 合金组织均匀, 基体和硬质相分布更加均匀, 所以, 提高了基体的耐磨性。这样, 在磨粒磨损过程中, 硬质相颗粒的剥落受到阻止, 基体和硬质相的结合和粘着更紧密, 从而提高了 NiCrWRe 合金的耐磨性。

### 3 结 论

(1) 通过稀土元素的添加, NiCrWRe 喷熔层粗大的条状组织均匀细化。稀土元素促进了喷熔层和基体之间原子的扩散, NiCrWRe 喷熔层与基体 45 号钢

形成了牢固的冶金结合, 提高了喷熔层结合强度。

(2) NiCrWRe 合金喷熔层耐磨性高于 NiCrW 合金喷熔层, 由于稀土元素的加入, 使 NiCrWRe 具有良好的耐磨性能, 磨损性能的差别主要取决于稀土对组织结构的影响, 以及磨粒磨损机制的三种方式协同作用的结果。

### 参考文献:

- [1] Hyung-Jun Kim, Soon-Young Hwang, Chang-Hee Lee, *et al.*. Assessment of wear performance of flame sprayed and fused Ni-based coatings[J]. *Surface and Coating Technology*, 2003, 172: 262-269.
- [2] 许斌, 冯承明, 张业民. 镍基碳化钨自熔合金喷焊层与硼化物层磨损特性的对比研究[J]. *摩擦学学报*, 1998, 18: 152-155.
- [3] 陈传忠, 李士同, 耿浩然, 等. Ni60A 等离子喷涂层的组织结构及其摩擦磨损特性[J]. *钢铁研究学报*, 1999, 11: 56-59.
- [4] Wang W L, Zhang Q B, Sun M L, *et al.*. Rare earth elements modification of laser-clad nickel-based alloy coatings[J]. *Applied Surface Science*, 2001, 174: 191-200.
- [5] Wei Yi, Changqiong Zheng, Peng Fan, *et al.*. Effect of rare earth on oxidation resistance of iron base fluxing alloy spray-welding coating[J]. *Journal of Alloys and Compounds*, 2000, 311: 65-68.
- [6] You Wang, Radovan Kovacevic, Jiajun Liu. Mechanism of surface modification of CeO<sub>2</sub> in laser remelted alloy spray coatings[J]. *Wear*, 1998, 221: 47-53.
- [7] Zhao Tao, Cai Xun, Wang Shunxing, *et al.*. Effect of CeO<sub>2</sub> on microstructure and abrasive wear behavior of laser-clad Ni/WC coating[J]. *Thin Solid Films*, 2000, 379: 128-132.
- [8] Zhenyu Zhang, Zhiping Wang, Bin Liang. Tribology properties of flame sprayed Fe-Ni-RE alloy coatings under reciprocating sliding[J]. *Tribology International*, 2006, 39: 1462-1468.
- [9] 张耀宗, 李延祥, 翟福宝, 等. 稀土对铁合金喷熔层的成分、组织及各种耐磨性的影响[J]. *洛阳工学院学报*, 1997, 18(3): 1-5.
- [10] Hui Wang, Weiming Xia, Yuansheng Jin. A Study on abrasive resistance of Ni-based coatings with a WC hard phase[J]. *Wear*, 1996, 195: 47-52.

作者简介: 张振宇, 男, 1972 年出生, 工学博士, 副教授。主要从事材料加工工程及新材料、纳米材料方面的科研和教学工作。发表论文 30 余篇。

Email: zlzhyu4281@163.com

transformation method, and a full kinematics model was established. And then a seam tracking controller based on fuzzy-gaussian neural network (FGNN) was described by applying a Gaussian function as an activation function, taking lateral slider position and heading angle of the robot as input signals and the adjusted angle for welding torch as output, a specialized learning architecture was used so that membership function could be tuned in real time by applying the backpropagation algorithm of FGNN controller. The experiment results show that the proposed controller has excellent tracing accuracy (within  $\pm 0.5$  mm), and can satisfy the requirement of practical welding project.

**Key words:** kinematics model; welding mobile robot; seam tracking; fuzzy neural network

**Friction stir spot welding process and mechanical properties of LY12 aluminum alloy** LIU Kewen<sup>1,2</sup>, XING Li<sup>1</sup>, KE Liming<sup>1</sup> (1. Schools of Material Science and Engineering, Nanchang Hangkong university, Nanchang 330063 China; 2. Jiangling Motor Company, Nanchang 330001, China). p21–24

**Abstract:** Friction stir spot welding (FSSW) is a relatively new solid state joining method, which is a variant of friction stir welding. The effect of the welding parameters on the shaping and mechanical properties of friction stir spot welded joint of 2 mm LY12 Al alloy was investigated. The results show that when the welding time is fixed, welding spot appearance is better with the increasing of the tool rotation speed, and it becomes worse with the decrease of the tool rotation speed and the welding time. The tensile shear strength of the spot increases firstly, and then reduces with the increasing of tool rotation speed. When the tool rotation speed is 950 r/min and welding time is 12 s, the maximum strength is up to 9.33 kN/spot. The microhardness show that the distribution of microhardness is high-low-sight higher-low-high along the centre of the keyhole, and the minimum value is in the heat affected zone, and the microhardness of plasticity zone was slightly lower than that of base metal.

**Key words:** Al alloy; friction stir spot welding; appearance of welding spot; mechanical properties

**Microstructure and wear-resistance property of NiCrWRe alloy sprayed coating** ZHANG Zhenyu<sup>1,2</sup>, WANG Zhiping<sup>2</sup>, LIANG Bunv<sup>1</sup> (1. Mechanical Engineering Department, Lanzhou Polytechnic College, Lanzhou 730050, China; 2. State Key Laboratory of New Nonferrous Materials, Lanzhou University of Technology, Lanzhou 730050, China). p25–28

**Abstract:** The NiCrWRe sprayed coating was prepared on the surface of 45 carbon steel by using flame spraying. The sprayed coating was characterized by abrasive wear resistance test, and compared with the NiCrW alloy coating. Scanning electron microscope, energy dispersion spectroscopy and X-ray diffraction were employed to analyze the morphologies of the coatings, as well as their phase structures. The bonding strength of coating/substrate interface was

tested by means of tensile strength. The results showed that the coating is firmly adhered to substrate, and contains the hard phase with higher proportion. Adding rare earth element can obviously increase the wear resistance of the coatings. In the given conditions, the wear resistance of NiCrWRe coating is much higher than that of NiCrW alloy coating.

**Key words:** rare earth; spray-fused coating; abrasive wear; wear resistance property

**Numerical simulation of arc reflection in plasma arc welding processing** YIN Fengliang, HU Shengsun, GAO Zhonglin, ZHU Shuangchun (College of Material Science and Engineering, Tianjin University, Tianjin 300072, China). p29–32, 90

**Abstract:** A three-dimensional mathematical arc model in keyhole PAW (plasma arc welding) process was established based on the mass, momentum and energy conservation equations. Magnetic-vector method was employed to solve the magnetic problem. A part of nozzle and tungsten electrode, as well as keyhole, were included into the model. The model was solved with ANSYS software. The simulated temperature was taken to indicate the arc reflection occurring in PAW processing. The plasma arc can be divided into main body, arc reflection and arc wake flame, which can be obtained from the simulated result. The effects of the keyhole dimension and offset between the arc axis and keyhole axis on the arc reflection were studied. The simulated results show that the arc reflection gets weaker and arc wake flame gets stronger with the increase of keyhole dimension, and a higher welding velocity to induce the offset between the arc axis and keyhole axis is necessary to the appearance of arc reflection, and the effects of welding current on the arc reflection are extended mainly through changing the keyhole dimension.

**Key words:** arc reflection; plasma arc welding; keyhole; simulation

**Nd:YAG laser welding of rapid-solidified heat-resistant aluminum alloy AA8009** DING Ronghui, LI Wenxian, WANG Richu, YU Kun (College of Materials Science and Technology, Center South University, Changsha 410083, China). p33–38

**Abstract:** Welding of rapid-solidified heat-resistant aluminum alloy AA8009 is very important to its application. Different welding parameter were used in the Nd:YAG laser butt welding of 1 mm thick AA8009 plate. The results show that, with the welding speed increase, and the total energy input decreases, and the cooling rate within the weld increases, and the weld microstructure are improved and changed from equilibrium state to non-equilibrium state microstructure. When the energy input is 8.15 J/mm, the tensile strength reaches 379.9 MPa, that the weld coefficient reached to 95% and the fracture happens at the boundary fusion zone.

**Key words:** rapid-solidified; heat-resistant aluminum alloy AA8009; Nd:YAG laser welding

**Effects of single and composite component oxides activating flux-**